

# NMR studies of nonplanar porphyrins. Part 1. Axial ligand orientations in highly nonplanar porphyrins



Craig J. Medforth,<sup>\*,a</sup> Cinzia M. Muzzi,<sup>a</sup> Kalyn M. Shea,<sup>a</sup> Kevin M. Smith,<sup>a</sup> Raymond J. Abraham,<sup>b</sup> Songling Jia<sup>c</sup> and John A. Shelnett<sup>c</sup>

<sup>a</sup> Department of Chemistry, University of California, Davis, California 95616, USA

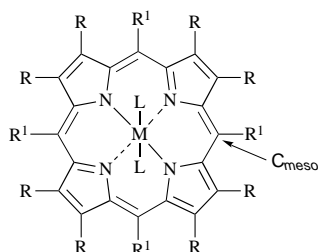
<sup>b</sup> School of Chemistry, University of Liverpool, PO Box 147, Liverpool, UK L69 3BX

<sup>c</sup> Fuel Science Department, Sandia National Laboratories, Albuquerque, New Mexico 87185-0710, USA

The ligand orientations in the nonplanar porphyrin complexes **1a–e** and **2a–e** have been investigated using molecular mechanics calculations and proton NMR spectroscopy. The minimum energy structures calculated for complexes **1a–e** show that the planes of the axial pyridine or imidazole ligands are orientated approximately parallel to the  $\text{Co}^{\text{III}}\text{-N}_{\text{porphyrin}}$  bonds, with the ligand ring planes being perpendicular to each other. For complexes **2a–e**, the planes of the axial ligands in the calculated minimum energy structures are orientated along the porphyrin *meso* carbon axis and the ligand ring planes are perpendicular to each other. Thus, for both series of complexes the planes of the axial ligands are orientated parallel to cavities formed by these very nonplanar porphyrins. Proton NMR studies suggest that structures similar to those obtained from the molecular mechanics calculations are retained in solution. In some complexes, hindered rotation of the axial ligands is also observed. Complexes **1a–e** and **2a–e** are unusual examples of the porphyrin conformation influencing the orientations of axial ligands and, as such, may be useful as models for studying ligand orientation effects in relation to biological systems.

## Introduction

Highly nonplanar porphyrins such as **1** and **2** (Fig. 1) have recently been employed in investigations aimed at determining how nonplanar conformational distortions affect the properties of porphyrins.<sup>1–7</sup> In the case of **1**, the high degree of nonplanarity exhibited by the porphyrin macrocycle has been found to cause a pronounced shift of the absorption maxima to longer wavelengths,<sup>1,3,4</sup> a significant decrease in the lifetime of the singlet excited state,<sup>3a</sup> and a lowering of the oxidation potential.<sup>1,2</sup> These findings have led to the suggestion that non-



- 1** R =  $\text{CH}_2\text{CH}_3$ , R<sup>1</sup> =  $\text{C}_6\text{H}_5$ , M = 2H  
**2** R = H, R<sup>1</sup> =  $\text{C}(\text{CH}_3)_3$ , M = 2H  
**a** M =  $\text{Co}^{\text{III}}$ , L = pyridine  
**b** M =  $\text{Co}^{\text{III}}$ , L = 3-phenylpyridine  
**c** M =  $\text{Co}^{\text{III}}$ , L = 3-chloropyridine  
**d** M =  $\text{Co}^{\text{III}}$ , L = 1-methylimidazole  
**e** M =  $\text{Co}^{\text{III}}$ , L = 4-phenylimidazole  
**f** M =  $\text{Co}^{\text{III}}$ , L = 4-methylpiperidine  
**3** R = H, R<sup>1</sup> = *ortho*- $\text{C}_6\text{H}_3\text{Cl}_2$ , M =  $\text{Co}^{\text{III}}$   
L = 1-methylimidazole  
**4** R = H, R<sup>1</sup> =  $\text{C}_6\text{H}_5$ , M =  $\text{Co}^{\text{III}}$   
**a** L = pyridine and chloride  
**b** L = imidazole  
**c** L = piperidine  
**d** L = 2-methylbenzimidazole  
**e** L = pyridine

Fig. 1 Structures and nomenclature for the porphyrin complexes discussed in this study

planar conformational distortions of tetrapyrroles in biological systems might have functional significance, for example in the photosynthetic reaction centre and light harvesting complex.<sup>1,8</sup>

In a recent communication, we noted that one unexpected consequence of the extremely nonplanar conformations adopted by complexes **1a–e** was the tendency of the planar axial ligands to orientate themselves along cavities formed by the nonplanar porphyrin macrocycle.<sup>9</sup> As it is believed that different orientations of the axial histidine ligands might be one mechanism for altering the oxidation potentials and spectroscopic properties of cytochromes,<sup>10</sup> we decided to explore in more detail the unusual ligand orientation effects seen in complexes **1a–e**, and to investigate the ligand orientations in complexes **2a–e** where the porphyrin adopts a different nonplanar conformation.<sup>6</sup> Attempts to crystallize complexes **1a–e** and **2a–e** have so far been unsuccessful, so, as in our earlier communication,<sup>9</sup> we have employed molecular mechanics calculations using a force-field that has been applied with considerable success to the prediction of crystal structures for many highly nonplanar porphyrins.<sup>4,6</sup> We then used proton NMR spectroscopy to investigate the solution conformations and dynamic properties of complexes **1a–e** and **2a–e**.

## Results and discussion

### Molecular mechanics calculations

Fig. 2 shows two views of the minimum energy structure calculated for complex **1a**. The porphyrin macrocycle in this complex clearly adopts a saddle conformation<sup>11</sup> in which alternate pyrrole rings are tilted up and down with respect to the porphyrin least-squares plane [Fig. 2(a)]. Similar saddle conformations are seen in the crystal structures of **1** (M = 2H,<sup>3b</sup>  $\text{Zn}^{\text{II}}$ ,<sup>1a</sup>  $\text{Cu}^{\text{II}}$ ,<sup>4b</sup>  $\text{Co}^{\text{II}}$ <sup>4b</sup> and  $\text{Ni}^{\text{II}}$ <sup>1b</sup>) and in the calculated minimum energy structures of these complexes.<sup>4b</sup> An analysis of the paramagnetic shifts in **1** (M =  $\text{Co}^{\text{II}}$ <sup>4b</sup>) also suggests that a saddle structure is retained in solution.<sup>12</sup>

The macrocycle conformation of **1a** does not seem to be

**Table 1** Structural parameters calculated for complexes **1a–f** and **2a–f**

	Co <sup>III</sup> –N <sub>ligand</sub> <sup>a/</sup> Å	Co <sup>III</sup> –N <sub>porphyrin</sub> <sup>a/</sup> Å	Angle to cavity (°) <sup>b</sup>	ΔE <sub>90°</sub> <sup>c/</sup> kJ mol <sup>-1</sup>
<b>1a</b>	1.99	1.92	10	123
<b>1b</b>	1.99	1.92	12	133
<b>1c</b>	1.99	1.92	14	123
<b>1d</b>	1.94	1.92	2	72
<b>1e</b>	1.93	1.92	3	79
<b>1f</b>	2.03	1.95	3	74
<b>2a</b>	2.00	1.89	0	128
<b>2b</b>	1.99	1.88	0	131
<b>2c</b>	1.99	1.88	0	124
<b>2d</b>	1.94	1.88	0	78
<b>2e</b>	1.94	1.88	0	79
<b>2f</b>	2.06	1.92	0	88

<sup>a</sup> Average bond length for all bonds of this type in the molecule.

<sup>b</sup> Average angle of the ligand plane with respect to the porphyrin cavity in the minimum energy structure. Calculated from the N<sub>porphyrin</sub>–Co<sup>III</sup>–N<sub>ligand</sub>–C<sub>ligand</sub> torsion angle for **1a–e** and **2a–e**, and from the N<sub>porphyrin</sub>–Co<sup>III</sup>–N<sub>ligand</sub>–H<sub>ligand</sub> torsion angle for **1f** and **2f**. <sup>c</sup> Energy difference between the minimum energy structure and an energy minimized structure with the plane of one ligand constrained at 90° to the porphyrin cavity.

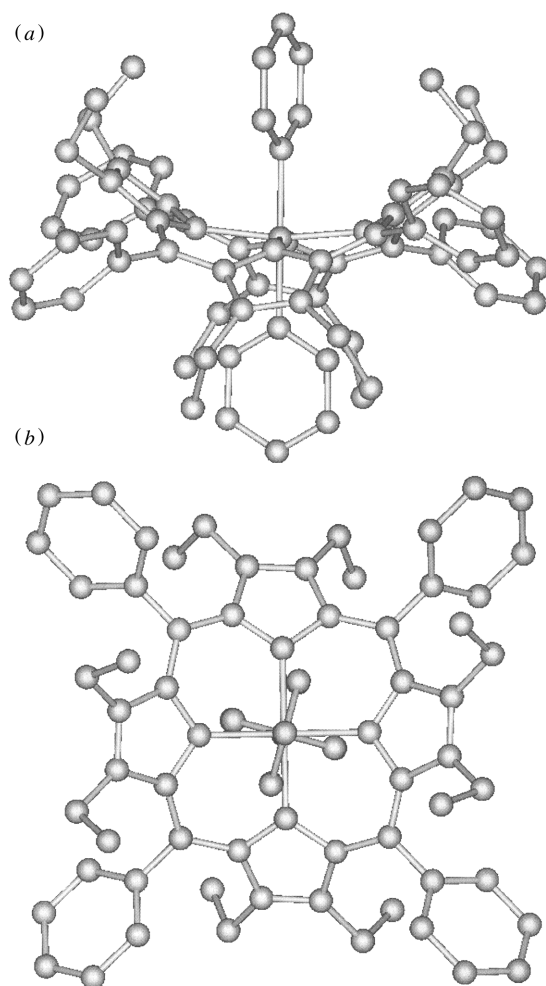


**Fig. 2** Two views of the minimum energy structure calculated for complex **1a**: (a) side view showing the highly nonplanar saddle structure of the porphyrin macrocycle. Note the cavities formed by the nonpolar macrocycle and the ethyl groups on the pyrrole rings. (b) A view looking down on to the plane of the porphyrin macrocycle, illustrating how the planes of the axial ligands are perpendicular to each other and nearly eclipse the Co<sup>III</sup>–N<sub>porphyrin</sub> bonds.

affected by the presence of the axial pyridine ligands. However, the orientations of the ligands are influenced by the conformation of the porphyrin macrocycle. The planes of the axial

ligands in **1a** are orientated approximately parallel to cavities formed by the nonplanar porphyrin macrocycle and the ethyl groups on the pyrrole rings, as shown in Fig. 2(a). Indeed, the planes of the axial ligands nearly eclipse the nitrogen atoms of the porphyrin pyrrole ring, making an angle of only 10° to the Co<sup>III</sup>–N<sub>porphyrin</sub> bond in the calculated structures [Fig. 2(b), Table 1]. Normally, an orientation of the planar axial ligands in which the ligand planes eclipse the Co<sup>III</sup>–N<sub>porphyrin</sub> bonds is disfavoured in porphyrin complexes because of close contacts between the porphyrin nitrogen atoms and the ligand protons (H-2 and H-6 in the case of pyridine) which point down into the porphyrin core.<sup>13</sup> For complex **1a**, the nearly eclipsed ligand orientation is most likely the result of steric constraints imposed by the nonplanar conformation of the porphyrin macrocycle. On this point, it is interesting to note that a ligand orientation similar to that seen for complex **1a** has proved difficult to obtain in bis(imidazole) iron(III) porphyrin systems,<sup>10</sup> and that this orientation of the axial histidine ligands in some cytochromes is believed to be maintained by the protein matrix.<sup>10a</sup>

An examination of the calculated structure of **1a** reveals that the porphyrin nitrogen atoms which lie along the same axis as the pyridine ligands are moved out of the porphyrin plane and away from the ligand hydrogens [Fig. 2(a)]. This displacement of the nitrogen atoms is an intrinsic feature of a saddle conformation,<sup>1a,1b,3b,4b</sup> and is no doubt one factor contributing to the unusual orientation of the ligands seen in the calculated structure of complex **1a**. Further molecular mechanics calculations showed only a small increase in the calculated energy of the complex when the structure was energy minimized with one ligand constrained to lie exactly parallel to the Co<sup>III</sup>–N<sub>porphyrin</sub> bonds (ΔE<sub>0°</sub> = 0.2 kJ mol<sup>-1</sup>). Constraining one ligand at an angle of 22.5° to the Co<sup>III</sup>–N<sub>porphyrin</sub> bonds also caused only a small increase in the calculated energy (ΔE<sub>22.5°</sub> = 2.1 kJ mol<sup>-1</sup>). This indicates a fairly flat potential for rotation of the axial pyridine ligands about the Co<sup>III</sup>–N<sub>ligand</sub> bond, which might reflect competition between the need to rotate the ligand out of the cavity to minimize N···H repulsions and the need to have the ligand plane parallel to the porphyrin cavity.

Constraining the plane of one ligand at 90° to the cavity so that it eclipses the other pair of Co<sup>III</sup>–N<sub>porphyrin</sub> bonds gave the highest energy ligand orientation (ΔE<sub>90°</sub> = 123 kJ mol<sup>-1</sup>) (Table 1). It was difficult to determine from the calculations alone which specific interactions were responsible for the observed energy increase because strain energy can be redistributed throughout the molecule. However, steric interactions between the porphyrin nitrogens and ligand protons will clearly play an important part, as the porphyrin nitrogen atoms on the axis perpendicular to the porphyrin cavity are displaced closer to the ligand protons by the saddle conformation of the porphyrin macrocycle [Fig. 2(a)].

The conformations of the porphyrin macrocycles and the orientations of the axial ligands calculated for the other pyridine complexes (**1b** and **1c**) and for the imidazole complexes (**1d** and **1e**) were similar to those seen for complex **1a**. The only significant difference was that the planes of the imidazole ligands were more centred in the cavities, as evidenced by smaller angles between the ligand plane and the Co<sup>III</sup>–N<sub>porphyrin</sub> bonds (Table 1). This effect is probably due to decreased N···H repulsions for the five-membered imidazole rings *versus* the six-membered pyridine rings. Decreased N···H repulsions should also lead to smaller ΔE values when one ligand is constrained at 90° to the porphyrin cavity, and this was indeed found to be the case (Table 1). Interestingly, in the case of complex **1f**, the planes of the chair-shaped 4-methylpiperidine ligands were also found to be orientated parallel to the porphyrin cavities in the calculated minimum energy structure.

The minimum energy structure calculated for complex **2a** is shown in Fig. 3. The calculated structure of this complex shows a strongly ruffled conformation of the porphyrin macrocycle in

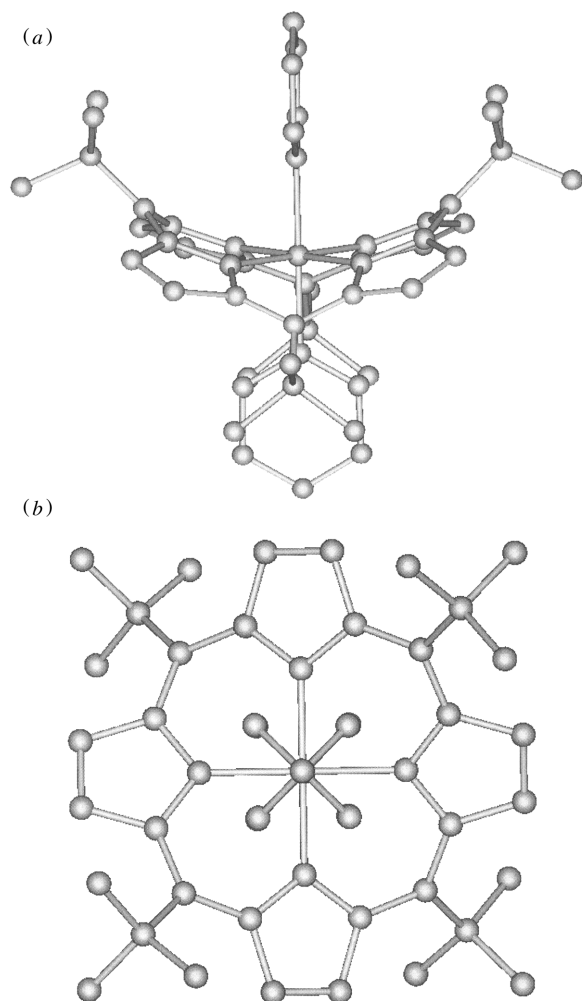


**Fig. 3** Two views of the minimum energy structure calculated for complex **2a**: (a) a side view showing the highly ruffled structure of the macrocycle and the cavities resulting from the nonplanar conformation and the *tert*-butyl substituents. (b) A view looking down on to the plane of the porphyrin macrocycle illustrating how the planes of the axial ligands are perpendicular to each other and are staggered with respect to the  $\text{Co}^{\text{III}}\text{-N}_{\text{porphyrin}}$  bonds.

which alternate pyrrole rings are twisted clockwise or anti-clockwise about the  $\text{Co}^{\text{III}}\text{-N}_{\text{porphyrin}}$  bonds [Fig. 3(a)]. A similar conformation of the porphyrin core is seen in the crystal structure of **2** ( $\text{M} = \text{Zn}^{\text{II}}$ ),<sup>14</sup> and is the minimum energy structure calculated for **2** ( $\text{M} = \text{Ni}^{\text{II}}$ ).<sup>6</sup> Therefore, the presence of the axial ligands in complex **2a** does not appear to affect the conformation of the porphyrin macrocycle.

The planes of the axial pyridine ligands in complex **2a** are orientated parallel to the axes containing the porphyrin *meso* positions, and are thus staggered (*i.e.* make an angle of  $45^\circ$ ) with respect to the  $\text{Co}^{\text{III}}\text{-N}_{\text{porphyrin}}$  bonds [Fig. 3(b)]. The planes of the axial pyridine ligands are also perpendicular to each other, and orientated parallel to the cavities formed by the nonplanar porphyrin macrocycle in a manner analogous to that seen in the calculated structure of complex **1a**. A similar conformation is seen for the other pyridine and imidazole complexes in this series (Table 1). The planes of the chair-shaped 4-methylpiperidine ligands in **2f** are also orientated parallel to the porphyrin cavities, as seen for complex **1f**.

Unlike the ligand orientation seen for complexes **1a–e**, the staggered orientation of the axial ligands in complexes **2a–e** effectively minimizes steric interactions between the ligand protons and the nitrogen atoms of the porphyrin pyrrole rings. This explains why the ligands in complexes **2a–e** are better aligned with the cavities than those in complexes **1a–e** (Table 1). Any deviations from an orientation exactly parallel to the cavity

**Table 2**  $^1\text{H}$  NMR data for complexes **1a–f** and **2a–f**<sup>a</sup>

	<b>1a</b>	<b>1b</b>	<b>1c</b>	<b>1d</b>	<b>1e</b>	<b>1f</b>
$\text{H}_{\text{ortho}}$	8.16	8.10 (4) <sup>b</sup>	8.17 (4)	8.21	8.12	8.25
$\text{H}_{\text{meta}}$	7.71	–7.67	7.70	7.70	–7.57	7.75
$\text{H}_{\text{para}}$	7.76	7.74	7.70	7.76	7.65	7.84
$\text{CH}_2$	2.23	2.20 (m)	2.29	2.18	2.11	2.44
$\text{CH}_3$	–0.05	–0.15 (4)	0.00	0.01	–0.07	0.41
$\Delta G^{\ddagger c}$	51	53	55	56	55	64
	<b>2a</b>	<b>2b</b>	<b>2c</b>	<b>2d</b>	<b>2e</b>	<b>2f</b>
$\beta\text{-H}$	9.22	9.29 (m)	9.28 (4)	9.17 (m)	9.15 (m)	9.61 (m)
$\text{Bu}^t$	1.49	1.53	1.55	1.62	1.54 (2)	2.16 (2)
$\Delta G^{\ddagger}$		>87	>81	57	61	65

<sup>a</sup> Average chemical shift (ppm) measured at ambient temperature as described in the Experimental section. <sup>b</sup> Figures in parentheses indicate the number of signals when macrocyclic inversion and ligand rotation are slow on the NMR timescale (m = multiple overlapping signals). <sup>c</sup> In  $\text{kJ mol}^{-1}$ . Estimated at the coalescence temperature using the standard equation.<sup>17</sup>

will increase  $\text{H}\cdots\text{N}$  interactions and other steric repulsions within the molecule. The same argument also explains the larger energy increase for **2a** ( $\Delta E_{22.5^\circ} = 15 \text{ kJ mol}^{-1}$ ) compared to **1a** ( $\Delta E_{22.5^\circ} = 2.1 \text{ kJ mol}^{-1}$ ) when one ligand is constrained at an angle of  $22.5^\circ$  to the porphyrin cavity. Interestingly,  $\Delta E_{90^\circ}$  for a given ligand was similar despite the very different structures and conformations of the complexes (Table 1).

Finally, the effect of different porphyrins and axial ligands on the  $\text{Co}^{\text{III}}\text{-N}_{\text{porphyrin}}$  and  $\text{Co}^{\text{III}}\text{-N}_{\text{ligand}}$  distances was examined. The  $\text{Co}^{\text{III}}\text{-N}$  distances for complexes **1a–e** and **2a–e** are summarised in Table 1, and calculated parameters for the complexes of **4** are given in the Experimental section. Shorter  $\text{Co}^{\text{III}}\text{-N}_{\text{porphyrin}}$  distances are normally observed for nonplanar porphyrins *versus* planar porphyrins,<sup>4b</sup> and the calculated  $\text{Co}^{\text{III}}\text{-N}_{\text{porphyrin}}$  distances for complexes **1a–e**, **2a–e** and **4b/4c/4e** show a similar trend: **1a–e**  $1.921 \pm 0.004$ , **2a–e**  $1.883 \pm 0.002$  and **4b/4c/4e**  $1.964 \pm 0.002$  Å. In contrast, the calculated  $\text{Co}^{\text{III}}\text{-N}_{\text{ligand}}$  distances do not vary significantly in porphyrins with the same axial ligands: **1a/2a/4e**  $1.997 \pm 0.003$ , **1d/2d/4b**  $1.940 \pm 0.005$  and **1f/2f/4c**  $2.040 \pm 0.019$  Å.

### $^1\text{H}$ NMR spectroscopy

Bis(amine) cobalt(III) complexes of **4** can be readily investigated by proton NMR spectroscopy because they are diamagnetic and exhibit ligand exchange which is slow on the NMR timescale.<sup>15</sup> The proton chemical shifts of complexes **1a–f** and **2a–f** (Table 2) show that these complexes are also diamagnetic. Furthermore, the addition of excess ligand indicated that ligand exchange was slow on the NMR timescale.

The methyl protons of **1a–e** and the *tert*-butyl protons of **2a–e** show large upfield shifts compared to complexes **1f** and **2f** which have the non-aromatic 4-methylpiperidine ligands. These chemical shift differences suggest that structures similar to those shown in Figs. 2 and 3 are retained in solution, with the methyl and *tert*-butyl protons pointing towards the face of the aromatic axial ligands and experiencing upfield ring current shifts. To confirm this hypothesis, ring current shifts were calculated for **1a** using the crystal structure of **1** ( $\text{M} = \text{Co}^{\text{II}}$ )<sup>4b</sup> with a pyridine ligand added using a standard geometry.<sup>15</sup> The pyridine ring current was simulated with the same dipole used to simulate the ring current in benzene ( $27.6 \text{ \AA}^3$ ).<sup>15</sup> The calculations gave an upfield shift of  $-0.33$  ppm for the methyl protons which is in reasonable agreement with a chemical shift difference of  $-0.46$  ppm between **1a** and **1f**. For **2a**, the minimum energy structure shown in Fig. 3 was used for the ring current calculations. The agreement between the observed shift ( $-0.67$  ppm) and calculated shift ( $-0.33$  ppm) was not quite as

good in this case. Overall, however, the results of the ring current calculations are consistent with structures similar to those shown in Figs. 2 and 3 being retained in solution.

Complexes **1a–e** and **2a–e** are unique in that there is direct experimental evidence suggesting that the ligand orientations are the same in solution as they are in the calculated (crystal) structures. For example, the crystal structure of complex **3**<sup>16</sup> shows that the 1-methylimidazole ligands adopt an orientation similar to that shown in Fig. 2. The planes of the axial imidazole ligands make an angle of 11° to the Co<sup>III</sup>–N<sub>porphyrin</sub> bond, and the planes of the axial ligands are perpendicular to each other. The ligands in **3** are likely forced into this orientation by the bulky chloro substituents at the *ortho* positions of the *meso* phenyl rings. However, there is no evidence that the ligand orientation seen in the crystalline state is retained in solution.

The dynamic behaviour of complexes **1a–f** and **2a–e** was also investigated using variable temperature proton NMR spectroscopy. At room temperature, only one signal was seen for each type of proton in complexes **1a–e**. However, upon cooling the complexes the methylene protons of the ethyl group became diastereotopic. The values of  $\Delta G^\ddagger$  for these dynamic processes (estimated at the coalescence temperature using the standard equation<sup>17</sup>) varied over a narrow range (51–56 kJ mol<sup>-1</sup>). Similar behaviour has been seen for other metal complexes of **1** and has been attributed to inversion of the nonplanar porphyrin macrocycle.<sup>1a</sup>

In the case of complexes **1b** and **1c**, additional protons also split into multiple signals as indicated in Table 2. The additional signals seen for complexes **1b** and **1c** suggest that, when inversion of the porphyrin macrocycle is slow on the NMR timescale, rotation of the axial ligands is also slow on the NMR timescale. In agreement with this suggestion, the number of signals seen for the porphyrin *ortho* protons (four) and methyl protons (four) in **1b** and **1c** is consistent with the number expected for the ligand orientation shown in Fig. 2. The absence of additional signals for the complexes **1d** and **1e** implies that ligand rotation is still fast on the NMR timescale for the imidazole ligands. This is in qualitative agreement with the  $\Delta E_{90^\circ}$  values obtained from the molecular mechanics calculations (Table 1), which are significantly lower for the imidazole ligands than for the pyridine ligands. Note that the symmetry of the pyridine ligand will preclude the observation of hindered ligand rotation in complex **1a**.

In contrast to complexes **1b** and **1c**, complexes **2b** and **2c** show multiple signals at ambient temperature (Table 2). This suggests that porphyrin inversion and ligand rotation are both slow on the NMR timescale. The number of signals seen for the pyrrole protons (four signals, two of which are coupled) also agrees with the number predicted for the ligand orientation shown in Fig. 3. The multiple proton signals do not coalesce upon heating, leading to the conclusion that the barriers for macrocyclic inversion in the tetra-*tert*-butyl porphyrins **2b** and **2c** are significantly higher than those in porphyrins **1b** and **1c** (which have substituents at all 12 peripheral positions). The proton NMR spectra of the imidazole complexes **2d** and **2e** are temperature dependent. The pyrrole and *tert*-butyl protons appear as single signals at room temperature but split into multiple signals upon cooling (Table 2).  $\Delta G^\ddagger$  for ligand rotation at the coalescence temperature was estimated to be 57 for **2d** and 61 kJ mol<sup>-1</sup> for **2e**. These values are considerably less than the barriers for rotation of the pyridine ligands, which is again consistent with the lower  $\Delta E_{90^\circ}$  values obtained from the molecular mechanics calculations (Table 1).

Hindered ligand rotation has previously been seen for iron(III) 5,10,15,20-tetraarylporphyrin complexes with sterically hindered axial ligands (e.g. 2-methylimidazole) or with bulky substituents on the *meso* phenyl ring.<sup>18</sup> Recently, hindered rotation of the axial ligands has also been noted for the cobalt(III) complex **4d** which has sterically hindered 2-methyl-

benzimidazole ligands.<sup>19</sup> Complexes **1a–e** and **2a–e** appear to be unique in this regard, as hindered ligand rotation does not require the presence of sterically hindered axial ligands or bulky porphyrin substituents but is a direct consequence of the unusually nonplanar structures exhibited by these porphyrins.

## Experimental

### Synthesis and <sup>1</sup>H NMR spectroscopy

300 MHz proton NMR spectra were recorded in CD<sub>2</sub>Cl<sub>2</sub> or CDCl<sub>3</sub> at ambient temperature (296 ± 4 K) and referenced to SiMe<sub>4</sub> or the solvent signal at 5.30 ppm (CHDCl<sub>2</sub>) or 7.26 ppm (CHCl<sub>3</sub>). The temperature control unit used in the variable temperature NMR experiments was calibrated using a sample of methanol.<sup>20</sup>

Complexes **1b–e** were prepared as described previously for **1a**.<sup>4b</sup> The complex **1** (M = Co<sup>II</sup>)<sup>4b</sup> was dissolved in chloroform, an excess of ligand was added, and the mixture was refluxed for 12 h open to the air. Oxidation of the cobalt(II) species could also be accelerated by adding a few drops of hydrogen peroxide (30% solution) to the refluxing mixture, whereupon complete oxidation was seen in a few minutes. In either case, the reaction mixture was cooled, washed with water, dried over sodium sulfate, and the solvent removed under vacuum. The residue was dissolved in a minimum volume of CH<sub>2</sub>Cl<sub>2</sub>, and the complexes crystallized (with an unknown anion) by addition of hexane. Complex **1f** could not be prepared using this procedure, and was generated in an NMR tube by adding an excess of iodine in CDCl<sub>3</sub> to **1** (M = Co<sup>II</sup>) in CDCl<sub>3</sub>, followed by addition of a slight excess of 4-methylpiperidine. Complex **1f** was also prepared by addition of a slight excess of 4-methylpiperidine to the chloro cobalt(III) complex of **1** in CDCl<sub>3</sub>. The latter was prepared by dissolving **1a** in chloroform and washing with the solution with 2 M hydrochloric acid.

Complexes **2a–e** were prepared by adding an excess of the ligand to **2**<sup>21</sup> in refluxing chloroform, followed by the addition of a saturated solution of cobalt(II) acetate in methanol. The reaction mixture was then refluxed until metal insertion and oxidation were complete, which was approximately 4 h. The reaction was worked-up using the same procedure described for complexes **1a–e**. This procedure did not work for complex **2f**, which was prepared in an NMR tube from **2c** via an exchange reaction with a large excess of 4-methylpiperidine.

### Molecular mechanics calculations

Molecular mechanics calculations using POLYGRAF software (Molecular Simulations, Inc.) were carried out and displayed on a Silicon Graphics Indigo<sup>2</sup> Extreme workstation. The force-field used in the calculations included force constants for bonds, angles, torsions and improper torsions, as well as van der Waals's and electrostatic contributions. It has been used with considerable success to predict the structures of nonplanar porphyrins.<sup>4,6</sup>

The force-field used in the present work is that described recently,<sup>6</sup> with the inclusion of published parameters for the Co<sup>III</sup>–N<sub>porphyrin</sub> bond.<sup>4</sup> Additional parameters were also included for the Co<sup>III</sup>–N<sub>ligand</sub> bond. The equilibrium Co<sup>III</sup>–N<sub>ligand</sub> bond distance for both pyridine and sp<sup>3</sup> nitrogen atoms was set to the same value used for the Co<sup>III</sup>–N<sub>porphyrin</sub> bond (1.90 Å). The Co<sup>III</sup>–N<sub>ligand</sub> force constants were taken as default values. The N<sub>ligand</sub>–Co<sup>III</sup>–N<sub>porphyrin</sub> equilibrium bond angle (90°) and force constant (36) were the same used for the porphyrin N<sub>porphyrin</sub>–Co<sup>III</sup>–N<sub>porphyrin</sub> angle. Finally, the Co<sup>III</sup>–N<sub>ligand</sub> torsion potential was set to zero.

The modified force-field was tested by comparing the crystal structures of complexes **4a**,<sup>22</sup> **4b**<sup>23</sup> and **4c**<sup>24</sup> with energy minimized structures calculated using the new force-field. The critical Co<sup>III</sup>–N<sub>ligand</sub> and Co<sup>III</sup>–N<sub>porphyrin</sub> distances calculated using the revised force-field were generally within the error limits of the crystallographic measurements (calculated values

in parentheses): **4a**<sup>22</sup> Co<sup>III</sup>-N<sub>porphyrin</sub> 1.978(8) (1.978) Co<sup>III</sup>-N<sub>ligand</sub> 1.976(12) (1.969) **4b**<sup>23</sup> Co<sup>III</sup>-N<sub>porphyrin</sub> 1.982(11) (1.974) Co<sup>III</sup>-N<sub>ligand</sub> 1.906(15) and 1.945(15) (1.959) **4c**<sup>24</sup> Co<sup>III</sup>-N<sub>porphyrin</sub> 1.978(5) (1.977) Co<sup>III</sup>-N<sub>ligand</sub> 2.060(3) Å (2.046 Å). The calculated macrocycle conformations were also the same as those seen in the crystal structures, with **4a** being slightly ruffled and **4b** and **4c** being essentially planar. Given the good agreement between the crystal and calculated structures for these cobalt(III) complexes, the revised force-field was then used to calculate energy minimized structures for the nonplanar porphyrin complexes **1a-f** and **2a-f**. The procedures used to obtain the minimum energy structures have been described previously.<sup>4,6</sup> Coordinates for the calculated structures can be obtained electronically from Professor John A. Shelnut (jasheln@sandia.gov).

Note added in proof: recent crystallographic studies of several complexes of porphyrin **1** support the conclusions reached in this work; M. W. Renner, K. M. Barkigia, D. Melamed, K. M. Smith and J. Fajer, *Inorg. Chem.*, 1996, **35**, 5120.

### Acknowledgements

Work performed at the University of California was supported by the National Science Foundation (CHE-93-05577; K. M. S.) and NATO (RG0218/87; R. J. A. and K. M. S.). Work performed at Sandia National Laboratories was supported by the US Department of Energy (DE-AC04-94AL8500; J. A. S.).

### References

- (a) K. M. Barkigia, M. D. Berber, J. Fajer, C. J. Medforth, M. W. Renner and K. M. Smith, *J. Am. Chem. Soc.*, 1990, **112**, 8851; (b) K. M. Barkigia, M. W. Renner, L. R. Furenlid, C. J. Medforth, K. M. Smith and J. Fajer, *J. Am. Chem. Soc.*, 1993, **115**, 3627.
- M. W. Renner, K. M. Barkigia, Y. Zhang, C. J. Medforth, K. M. Smith and J. Fajer, *J. Am. Chem. Soc.*, 1994, **116**, 8582.
- (a) S. Gentemann, C. J. Medforth, T. P. Forsyth, D. J. Nurco, K. M. Smith, J. Fajer and D. Holten, *J. Am. Chem. Soc.*, 1994, **116**, 7363; (b) A. Regev, T. Galili, C. J. Medforth, K. M. Smith, K. M. Barkigia, J. Fajer and H. Levanon, *J. Phys. Chem.*, 1994, **98**, 2520.
- (a) J. A. Shelnut, C. J. Medforth, M. D. Berber, K. M. Barkigia and K. M. Smith, *J. Am. Chem. Soc.*, 1991, **113**, 4077; (b) L. D. Sparks, C. J. Medforth, M.-S. Park, J. R. Chamberlain, M. R. Ondrias, M. O. Senge, K. M. Smith and J. A. Shelnut, *J. Am. Chem. Soc.*, 1993, **115**, 581.
- K. M. Kadish, E. V. Caemelbecke, P. Bolas, F. D'Souza, E. Vogel, M. Kisters, C. J. Medforth and K. M. Smith, *Inorg. Chem.*, 1993, **32**, 4177.
- W. Jentzen, J. D. Hobbs, M. C. Simpson, K. K. Taylor, T. Ema, N. Y. Nelson, C. J. Medforth, K. M. Smith, M. Veyrat, M. Mazzanti, R. Ramassel, J.-C. Marchon, T. Takeuchi, W. A. Goddard III and J. A. Shelnut, *J. Am. Chem. Soc.*, 1995, **117**, 11 085.
- S. Gentemann, C. J. Medforth, T. Ema, N. Y. Nelson, K. M. Smith, J. Fajer and D. Holten, *Chem. Phys. Lett.*, 1995, **245**, 441.
- (a) J. Fajer, *Chem. Ind.*, 1991, 869; (b) M. O. Senge, *J. Photochem. Photobiol. B: Biol.*, 1992, **16**, 3.
- C. J. Medforth, C. M. Muzzi, K. M. Smith, R. J. Abraham, J. D. Hobbs and J. A. Shelnut, *J. Chem. Soc., Chem. Commun.*, 1994, 1843.
- (a) F. A. Walker, B. H. Huynh, W. R. Scheidt and S. R. Osvath, *J. Am. Chem. Soc.*, 1986, **108**, 5288; (b) M. K. Safo, G. P. Gupta, F. A. Walker and W. R. Scheidt, *J. Am. Chem. Soc.*, 1991, **113**, 5497; (c) M. K. Safo, G. P. Gupta, C. T. Watson, U. Simonis, F. A. Walker and W. R. Scheidt, *J. Am. Chem. Soc.*, 1992, **114**, 7066; (d) M. K. Safo, F. A. Walker, A. M. Raitisring, W. P. Walters, D. P. Dolata, P. G. Debrunner and W. R. Scheidt, *J. Am. Chem. Soc.*, 1994, **116**, 7760.
- W. R. Scheidt and Y. J. Lee, *Struct. Bonding (Berlin)*, 1987, **64**, 1.
- C. J. Medforth, J. D. Hobbs, M. R. Rodriguez, R. J. Abraham, K. M. Smith and J. A. Shelnut, *Inorg. Chem.*, 1995, **34**, 1333.
- D. M. Collins, R. Counryman and J. L. Hoard, *J. Am. Chem. Soc.*, 1972, **94**, 2066.
- M. O. Senge, T. Ema and K. M. Smith, *J. Chem. Soc., Chem. Commun.*, 1995, 733.
- R. J. Abraham and C. J. Medforth, *Magn. Reson. Chem.*, 1987, **25**, 432.
- H. Bang, J. O. Edwards, J. Kim, R. G. Lawler, K. Reynolds, W. J. Ryan and D. A. Sweigart, *J. Am. Chem. Soc.*, 1992, **114**, 2843.
- R. J. Abraham, J. Fisher and P. Loftus, *Introduction to NMR Spectroscopy*, Wiley, Chichester, 1988.
- (a) H. Zhang, U. Simonis and F. A. Walker, *J. Am. Chem. Soc.*, 1990, **112**, 6124; (b) F. A. Walker and U. Simonis, *J. Am. Chem. Soc.*, 1991, **113**, 8652.
- M. Nakamura and A. Ikezaki, *Chem. Lett.*, 1995, 733.
- A. L. van Geet, *Anal. Chem.*, 1970, **42**, 679.
- T. Ema, M. O. Senge, N. Y. Nelson and K. M. Smith, *Angew. Chem., Int. Ed. Engl.*, 1994, **33**, 1879.
- T. Sakurai, K. Yamamoto, N. Seino and M. Katsuta, *Acta Crystallogr., Sect. B*, 1975, **31**, 2514.
- K. W. Lauher and J. A. Ibers, *J. Am. Chem. Soc.*, 1974, **96**, 4447.
- W. R. Scheidt, J. A. Cunningham and J. L. Hoard, *J. Am. Chem. Soc.*, 1973, **95**, 8289.

Paper 6/03412H  
Received 16th May 1996  
Accepted 18th November 1996